

# Physical evolution of a bentonite buffer during 18 years of heating and hydration



María Victoria Villar<sup>a,\*</sup>, Rubén Javier Iglesias<sup>a</sup>, José Luis García-Siñeriz<sup>b</sup>, Antonio Lloret<sup>c</sup>, Fernando Huertas<sup>d</sup>

<sup>a</sup> Centro de Investigaciones Energéticas, Medioambientales y Tecnológicas (CIEMAT), Avd. Complutense 40, 28040 Madrid, Spain

<sup>b</sup> Amberg Infraestructuras S.A., Avda. de la Industria 37-39, 28108 Alcobendas, Spain

<sup>c</sup> Universitat Politècnica de Catalunya (UPC), Jordi Girona 1-3, 08034 Barcelona, Spain

<sup>d</sup> formerly ENRESA, Emilio Vargas 7, 28043 Madrid, Spain

## ARTICLE INFO

### Keywords:

Radioactive waste disposal  
Barriers  
Bentonite  
Swelling  
Partial saturation  
Adsorbed water density

## ABSTRACT

The FEBEX in situ experiment was a full-scale test reproducing the near-field of an underground nuclear waste repository. It was performed in a gallery excavated in granite, two heaters simulated the thermal effect of the waste canisters and a bentonite barrier composed of highly-compacted blocks surrounded them, acting as buffer between the heaters and the crystalline host rock. The barrier slowly hydrated with the natural incoming groundwater. The bentonite and rock were instrumented and the sensors provided information about the state of the barrier. Half of the experiment was dismantled after five years of operation (partial dismantling), and the other half was left running for subsequent thirteen years before the complete, final dismantling. During both the partial and the final dismantling numerous samples of bentonite were taken for the on-site determination of dry density and water content. This work compares the physical state of the bentonite barrier after two different periods of time, drawing conclusions about the performance of the barrier and the factors affecting its saturation rate and evolution.

The physical state of the barrier was mostly conditioned by the heating and hydration processes, although at some points it was affected by installation particularities. The dry density gradients generated proved to be persistent, and maybe largely irreversible, since they were already observed after five years of operation and remained for another thirteen years, despite the fact that the degree of saturation at the end of the experiment was overall quite high. These gradients did not impair the performance of the barrier and its sealing ability.

To properly compute the bentonite degree of saturation the differences between the microstructural and macrostructural water density have to be taken into account, and this is essential for the proper estimation of the time needed for full saturation of the barrier. In any case, the water content changes evidenced the slowing down of the hydration rate over time.

## 1. Introduction

The safety of the deep geological repository concepts for nuclear waste disposal is based on the superposition of barrier systems, among which are the canister and the buffer, usually a clay-based barrier (Ericsson, 1999; Sellin and Leupin, 2013). The clay barrier has the multiple purpose of providing mechanical stability to the gallery and canister, delaying the access of water to the waste package and retaining/retarding the migration of radionuclides eventually released from a deteriorating canister.

In this context, the aim of the FEBEX (Full-scale Engineered Barriers

Experiment) Project was to study the behaviour of components in the near-field for a high-level radioactive waste (HLW) repository in crystalline rock. The project was designed to simulate in the extent possible the Spanish reference concept for disposal of radioactive waste in crystalline rock (AGP Granito): the waste canisters are placed horizontally in drifts and surrounded by a clay barrier constructed from highly-compacted bentonite blocks (ENRESA, 1995). As part of this project, the FEBEX in situ test aimed to reproduce the conditions of the engineered barrier system in an underground repository of nuclear waste. It was a full-scale test performed at the Grimsel Test Site (GTS, Switzerland), an underground laboratory managed by NAGRA, the

\* Corresponding author.

E-mail addresses: [mv.villar@ciemat.es](mailto:mv.villar@ciemat.es) (M.V. Villar), [rubenjavier.iglesias@ciemat.es](mailto:rubenjavier.iglesias@ciemat.es) (R.J. Iglesias), [jgarciasineriz@amberg.es](mailto:jgarciasineriz@amberg.es) (J.L. García-Siñeriz), [antonio.lloret@upc.edu](mailto:antonio.lloret@upc.edu) (A. Lloret).

<https://doi.org/10.1016/j.enggeo.2019.105408>

Received 24 July 2019; Received in revised form 23 October 2019; Accepted 11 November 2019

Available online 13 November 2019

0013-7952/ © 2019 Elsevier B.V. All rights reserved.

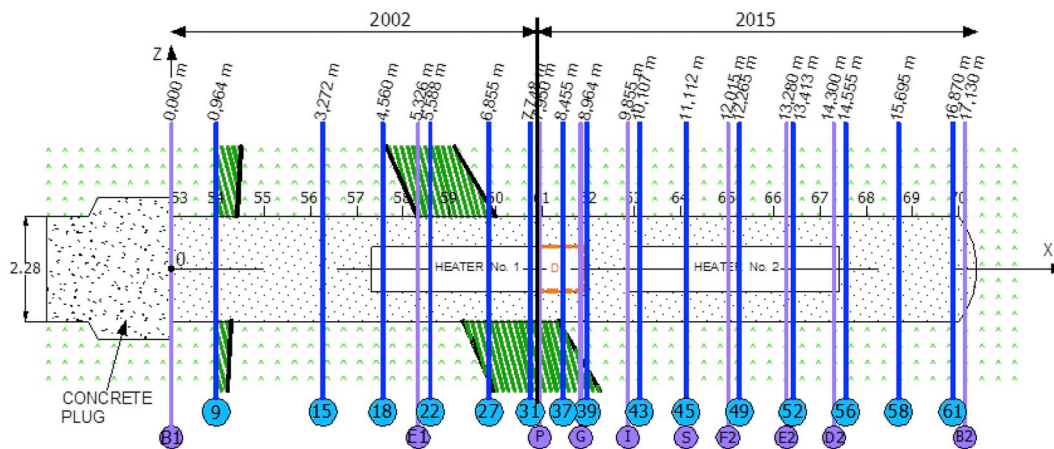


Fig. 1. Schematic representation of the FEBEX gallery with indication of the sampling sections used for onsite analyses in 2002 (sections S9–S31) and 2015 (S37–S61) and of the instrumented sections (letters). The origin of x-coordinates (0) and the dummy canister installed in 2002 (D) are shown.

Swiss agency for nuclear waste management. A 70-m long and 2.28-m diameter gallery was excavated across the Aare granite in 1995. The thermal effect of the heat-generating canisters was simulated by two heaters of dimensions and weight analogous to the Spanish reference waste containers. They were placed inside a perforated steel liner installed concentrically with the gallery and separated one from the other by a distance of 1.0 m. The engineered barrier around these heaters was composed of highly compacted FEBEX bentonite blocks. The testing area was 17.4 m long and it was closed by a 2.7-m thick keyed concrete plug (Fig. 1). Fig. SM-1 (in Supplementary Material) shows the heterogeneous geology and hydrogeological conditions along the gallery, in particular the thick and highly conductive lamprophyre dyke that crossed the first half of the experiment (also shown in Fig. 1), but also the dense fracture system at the dead-end of the gallery (Pardillo et al., 1997; Martínez-Landa and Carrera, 2005).

The test was designed and started in the framework of the FEBEX project, financed by ENRESA, the Spanish agency for nuclear waste management, and the European Commission. Details of the FEBEX project and of the in situ test design and operation can be found in ENRESA (2006) and Gens et al. (2009).

The heating stage of the in situ test began in 1997. The power of the heaters was adjusted so that to keep the temperatures at the liner surface at 100 °C, and the clay barrier slowly hydrated under natural groundwater inflow conditions. After five years, the heater closer to the gallery entrance (Heater #1) was switched off and extracted, along with all the bentonite and instruments preceding and surrounding it. This is known as the “partial dismantling”, which was described in Bârcena et al. (2003). The buffer and all components were removed up to a distance of 2 m from the front of Heater #2 to minimise disturbance of the non-dismantled area. A dummy steel cylinder with a length of 1 m was inserted in the void left by Heater #1 in the centre of the buffer. Additional sensors were also introduced in boreholes drilled in the buffer parallel to the drift. The remaining part of the experiment was sealed with a shotcrete plug and a second operational phase started. The test continued running until April 2015, when heater #2 was switched off. The final complete dismantling of the experiment was undertaken, and the buffer removal and sampling took place between May and August 2015, as described in García-Siñeriz et al. (2016).

Although other similar in situ tests have been carried out and dismantled (e.g. Bernier and Neerdael, 2007; Karnland et al., 2011; García-Siñeriz et al., 2015; Mokni and Barnichon, 2016), the FEBEX in situ test is the longest one dismantled until now. The samples retrieved during the final dismantling had been exposed to repository conditions for 18 years, allowing for a significant maturation of the bentonite and for possible modifications that could have not been observed in shorter experiments. Furthermore, the fact that part of the barrier had been

dismantled after a shorter period of time allowed to have an intermediate check of the conditions of the barrier and therefore assess its evolution. The FEBEX large-scale test is also the only one of its kind in which a not predominantly sodic bentonite was used as barrier material.

During the two dismantling operations many bentonite samples were taken for analysis on site and for thermal, hydro-mechanical, geochemical and mineralogical characterisation in different laboratories (Villar et al., 2005; Villar, 2006; Villar and Lloret, 2007; Villar et al., 2016, 2018). The research presented here compares the results obtained during the partial and final dismantling about the physical state of the bentonite barrier, taking also into account the information provided by the sensors during the operational phase. In this way, conclusions have been drawn about the performance of the barrier, its saturation rate, evolution over time and the factors affecting these processes.

## 2. The bentonite barrier

The clay barrier was made of FEBEX bentonite, which was a 900-t batch of bentonite extracted from the Cortijo de Archidona quarry (Almería, Spain) and processed in 1996 for the FEBEX project. The processing consisted in homogenisation, air-drying and manual removing of volcanic pebbles on-site and, at the factory, crumbling, drying in a rotary oven at temperatures between 50 and 60 °C and sieving through a 5-mm mesh. The physico-chemical properties of the FEBEX bentonite, as well as its most relevant thermo-hydro-mechanical and geochemical characteristics obtained during the FEBEX project were summarised in e.g. ENRESA (2006), Lloret and Villar (2007). This material was also used in laboratory tests for the EU-financed NF-PRO and PEBS projects (Villar and Gómez-Espina, 2009) and was distributed over the years to different laboratories to be used in different projects.

The montmorillonite content of the FEBEX bentonite is  $92 \pm 4$  wt% and it also contains variable quantities of quartz ( $2 \pm 1$  wt%), plagioclase ( $3 \pm 1$  wt%), K-felspar (traces), calcite (1 wt%) and cristobalite–tridymite ( $2 \pm 1$  wt%). The cation exchange capacity is  $98 \pm 2$  meq/100 g, the main exchangeable cations being calcium ( $33 \pm 2$  meq/100 g), magnesium ( $33 \pm 3$  meq/100 g) and sodium ( $28 \pm 1$  meq/100 g).

The swelling pressure ( $P_s$ , MPa) of FEBEX samples flooded with deionised water up to saturation at room temperature and constant volume conditions can be related to dry density ( $\rho_d$ , g/cm<sup>3</sup>) through the following equation (Villar, 2002):

$$\ln P_s = 6.77\rho_d - 9.07 \quad (1)$$

Hence, for the average dry density of the barrier (1.6 g/cm<sup>3</sup>) the

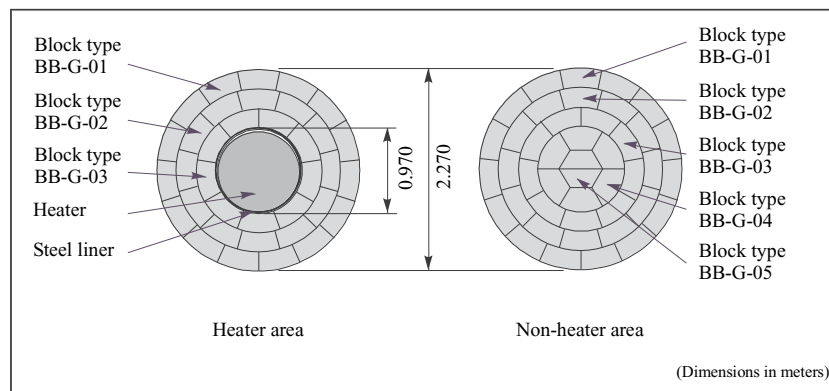


Fig. 2. Geometry of the clay barrier in the FEBEX in situ test at GTS (ENRESA, 2006).

expected swelling pressure would be about 6 MPa. The hydraulic conductivity of the bentonite is also exponentially related to its dry density, and under the same conditions mentioned in the previous paragraph, it would be about  $5 \cdot 10^{-14}$  m/s.

To build the clay barrier, various types of bentonite blocks were manufactured to obtain 12.5-cm thick circular crown sectors. The blocks were produced by uniaxial compaction of the FEBEX clay with its hygroscopic water content (~14%) at pressures of between 40 and 45 MPa, which resulted in dry densities of 1.69–1.70 g/cm<sup>3</sup>. The initial dry density of the blocks was selected by taking into account the probable volume of the construction gaps and the need to have a barrier with an average dry density of 1.60 g/cm<sup>3</sup> (ENRESA, 2006).

The blocks were manually arranged in 12.5-cm thick vertical slices consisting of concentric rings. In the heater areas the interior ring was in contact with the steel liner, whereas in the non-heater areas a core of bentonite blocks replaced the heaters (Fig. 2). The thickness of the bentonite barrier in the heater areas was 65 cm (distance from liner to granite). The total mass of the bentonite barrier was 115.7 t.

Following the same terminology used during installation of the experiment, the term bentonite “slice” refers to the vertical slices of bentonite blocks as they were installed. These were numbered during the installation of the barrier in 1996 as they were put in place: from slice 1, at the back of the gallery, to slice 136, the last one installed, at the front of the barrier in contact with the first concrete plug. The term “section” refers to the vertical sampling sections in which samples of any kind were taken during dismantling. They were numbered from the entrance of the gallery towards the back of it, and the numbering started in the first dismantling. Hence, sampling Sections S1 to S30 were sampled in 2002, and sampling Sections S31 to S61 were sampled in 2015 (Fig. 1).

### 3. Online measurements during the operational phase and dismantling

A total of 632 instruments, located in both the bentonite buffer and the host rock, were initially installed in some sections (Fig. 1). A Data Acquisition and Control System located in the service area of the FEBEX drift collected the data provided by the instruments. This system recorded and stored information from the sensors and also controlled the power supplied to the electrical heaters to maintain a constant temperature at the liner/bentonite interface. The instruments monitored relevant parameters such as temperature, humidity, total and pore pressure, displacements, etc. and their characteristics and positions were fully described in Fuentes-Cantillana and García-Siñeriz (1998).

After an initial 2-month calibration phase the heating system was left to regulate the power to reach and maintain 100 °C maximum at the liner-barrier contact. After the first year the power needed was about 1940 W for Heater #1 and 2170 W for Heater #2, because the latter was totally surrounded by conductive materials, whereas Heater #1 had in

front the open gallery. Then the power required at Heater#1 started to increase slowly until its decommissioning, when it reached 2160 W. Approximately two years after the start of the experiment the power supplied to Heater #2 started to increase slightly too and maintained the trend until decommissioning of Heater #1, reaching a value of around 2300 W. The increase over time of the needed power was caused by a thermal conductivity increase associated to the bentonite hydration. The temperatures measured in the barrier just before the partial dismantling in 2002 are shown in Fig. 3. The steady temperatures in the bentonite were between 100 °C and 36 °C in the sections around the heaters – with maximum values around their middle part –, 20 °C in the contact with the concrete plug and around 22 °C at the back of the gallery.

There was an increase in the power of Heater #2 of about 5% (~100 W) during approximately two months after the disconnection of Heater #1. Afterwards, the power supplied tended to increase around 40 W per year to keep 100 °C at the bentonite contact. The power supplied to Heater#2 was of 2796 W just before switching it off for final decommissioning, with a total increase in power from day 56 (24/04/97) up to the switching off day of about 18.5%. However, after the partial dismantling in 2002 the temperatures at the front of Heater #2 decreased as a result of Heater #1 removal. At the back of the gallery the temperature in the bentonite did not change during the 18-year operation, but around Heater #2, in the parts of the barrier closest to it, the temperature slightly increased from 2002 to 2015 (Fig. 4), which is probably the result of the increase in water content (analysed below), and consequently in thermal conductivity, occurred during the further 13 years of heating and hydration.

The relative humidity in the pores of the bentonite, which is related to the degree of water saturation of the clay, measured just before dismantling in 2002 is shown in Fig. 5. The initial relative humidity of

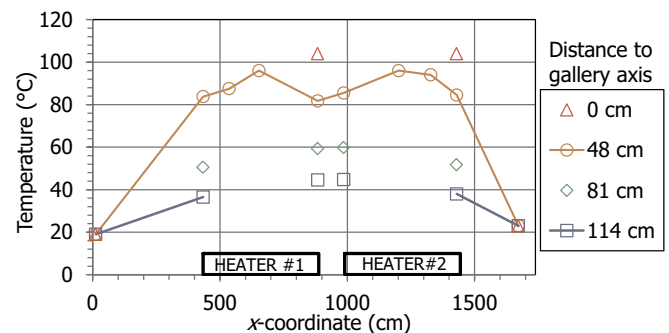


Fig. 3. Temperatures measured along the bentonite barrier at different distances from the gallery axis (indicated in the legend) before dismantling in 2002 (data from Bárcena et al., 2006, most points are the average of four measurements taken at the same radial distance).

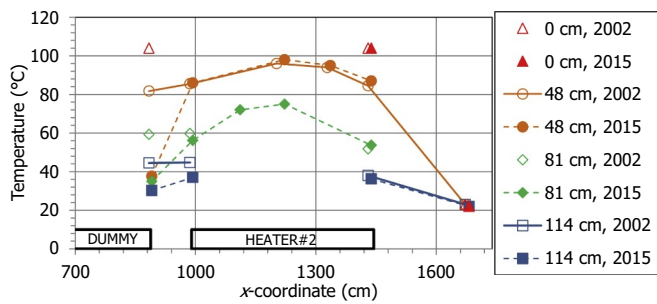


Fig. 4. Temperatures measured along the bentonite barrier around Heater #2 at different distances from the gallery axis (indicated in the legend) before partial dismantling in 2002 (empty symbols, data from [Bárcena et al., 2006](#)) and final dismantling in 2015 (filled symbols, data from [Martínez et al., 2016](#)).

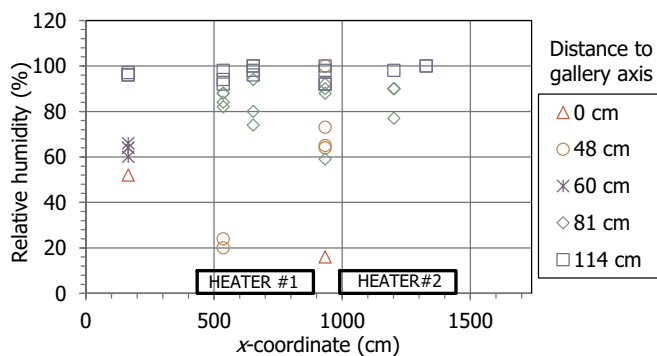


Fig. 5. Relative humidity measured along the bentonite barrier at different distances from the gallery axis (indicated in the legend) before dismantling in 2002 (data from [Bárcena et al., 2006](#)).

the bentonite blocks just after installation in 1997 was around 40% ([Bárcena et al., 2006](#)). In 2002 all the sensors located close to the granite recorded values close to 100%, i.e. very low to null suction (considering the 3% sensor accuracy in this suction range), corresponding to conditions in the bentonite close to full saturation. The sensors located at about 30 cm from the granite into the barrier (distance to gallery axis 81 cm), recorded values mostly above 80%, indicating the inward progress of hydration, but also the arrival of water in the vapour phase from hot inner parts of the barrier ([Gens et al., 2009](#)), where the temperatures were between 50 and 60 °C (see [Fig. 3](#)). In fact, close to the heaters the relative humidity after five years of heating and hydration was well below the initial value, which reflected the intense drying occurred as a result of the high temperature. After the transient associated with partial dismantling, the relative humidity in the buffer resumed a slow increase in all but the outer ring of the buffer which was already highly saturated.

At the time of dismantling in 2015, five out of the six relative humidity sensors still working, recorded values of 100%. These were all located at less than 20 cm from the granite. A sensor at 10 cm from the surface of Heater #2 in section S (S45) recorded a value of 60% ([Martínez et al., 2016](#)).

The total pressure recordings –which are also related to the degree of saturation, since swelling pressure is assumed to increase with increasing degree of saturation– showed mostly an increasing trend both in 2002 and in 2015 ([Fig. 6](#)). At the moment of dismantling in 2002, the pressure exerted by the bentonite against the concrete plug closing the gallery was about 1 MPa at the axis of the gallery and between 3.6 and 4.6 MPa in the middle part of the barrier (section B1, [Fig. 7](#) left). The sensors located close to the heater recorded values below 2 MPa (sections E1, I, E2) whereas those at the bentonite/granite contact recorded values between 2 and 5 MPa in 2002 that remained constant or increased to 6 MPa during the whole operation time. Also at locations

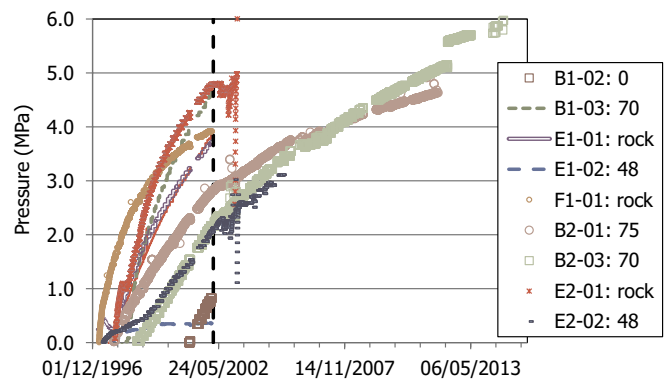


Fig. 6. Total pressure evolution measured inside the bentonite from the beginning of operation (see [Fig. 1](#) for location of sections). The distance of the sensor from the gallery axis is indicated in cm (rock: granite/bentonite contact), the dotted vertical line indicates the start of partial dismantling.

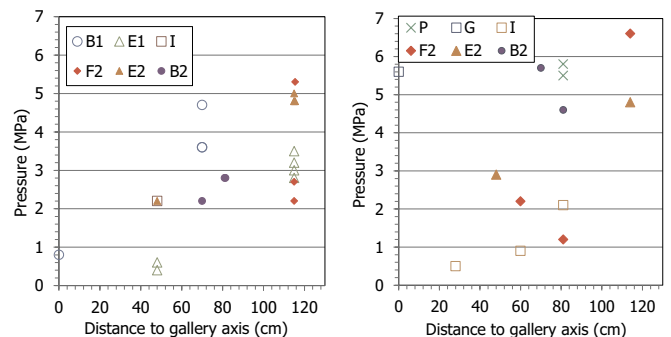


Fig. 7. Total pressures measured in the bentonite barrier (the location of the sections indicated in the legend is shown in [Fig. 1](#)) before partial dismantling in 2002 (left, data from [Bárcena et al., 2006](#)) and before final dismantling in 2015 (right, data from [Martínez et al., 2016](#)).

further away from the heater, at the back of the gallery (section B2, [Fig. 7](#) right), total pressure values between 5 and 6 MPa (and even higher at the contact bentonite/rock) were recorded in 2015. These values would correspond to the swelling pressure of saturated bentonite of density 1.58–1.61 g/cm<sup>3</sup> (Eq. 1). However, the sensors located in the intermediate ring of sections around the heater recorded in 2015 values just slightly above 2 MPa, which were far from the equilibrium pressure expected for the average dry density of the barrier and would indicate that saturation had not been reached.

The sensors continued working during the dismantling works. Upon switching off the heaters the temperatures dropped to values suitable for manual operation at all points of the barrier in less than three weeks. [Fig. 8](#) shows the drop in temperature recorded around Heater #1 when switched off in 2002 and around Heater #2 when switched off in 2015. The temperatures dropped more quickly and to lower values in the case of Heater #2, because when Heater #1 was switched off, Heater #2 continued heating the system, whereas there was no additional heat source during the second dismantling.

As a result of this temperature reduction and change in the thermal field, there was a redistribution of water in the clay buffer, by inversion of the two-phase flow mechanism. A significant and fast increase in relative humidity close to Heater #1 and a decrease of RH values in the intermediate bentonite ring were observed when the heater was switched off in 2002 ([Villar et al., 2005](#); [Villar et al., 2012](#)). It is probable that a similar process took place when Heater #2 was switched off in 2015, but there were no relative humidity sensors working to confirm this ([Villar et al., 2018](#)).

The temperature drop also made the already low pore pressures in

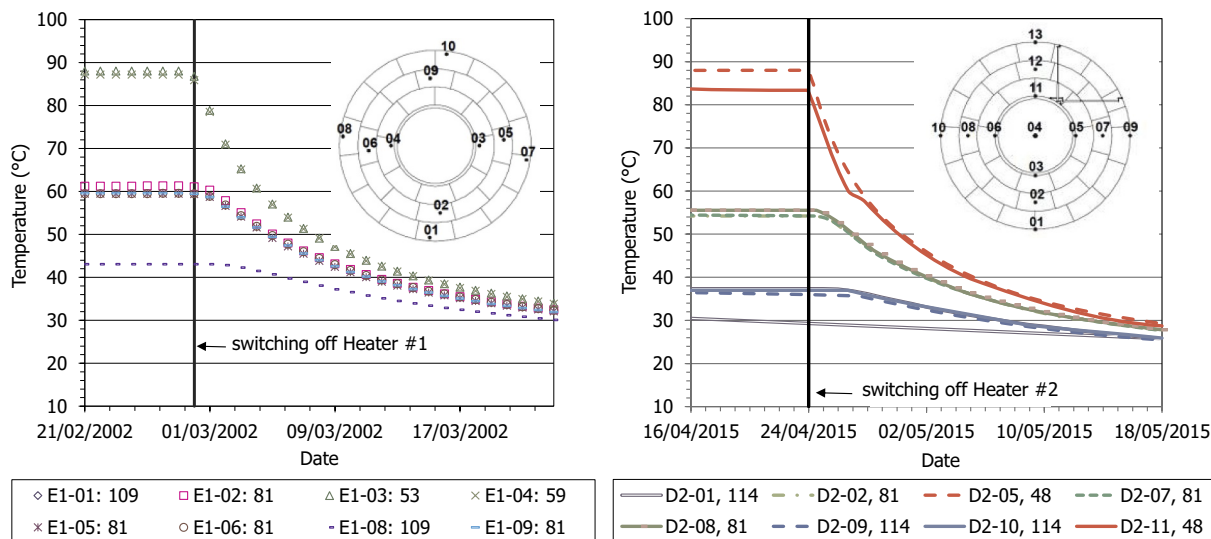


Fig. 8. Evolution of temperature in section E1 (2002) and D2 (2005) upon switching off heaters (reference of sensors and distances to gallery axis in cm indicated in the legends; location of sections in Fig. 1).



Fig. 9. Appearance of the core of the barrier in cold zones after 5 years (left, slice 118, section S13) and 18 years (right, slice 17, section S57–S58).

the bentonite decrease and, as the sensors' location was approached during dismantling, the pore pressure values plunged to zero. This behaviour was consistent with the recordings provided by the total pressure cells and reflected the buffer decompression. The recordings during the plug demolition of the total pressure cells placed between the shotcrete plug and the bentonite are shown in Fig. SM-2 of the Supplementary Material.

#### 4. Engineered barrier dismantling

The bentonite dismantling works started after the heater had been switched off for three months in 2002 and only 14 days in 2015. The experience gained in 2002 made that the final dismantling run more smoothly and showed less relevant difficulties, particularly for the concrete plug demolition. The bentonite dismantling and sampling works took two months in 2002 and three months in 2015.

During the two dismantling operations numerous samples of bentonite were taken in selected vertical sections evenly distributed along the gallery for the onsite determination of their dry density and water content (see Fig. 1 for location of these sampling sections). Additionally, the blocks' dimensions were measured, as well as the x-coordinate changes for the block slices. The results of the onsite measurements and other field observations concerning the state of the bentonite barrier after the first five operational years were reported in Villar et al. (2005) and Villar (2006), whereas for the final dismantling

after 18 years these results were given and analysed in Villar et al. (2016, 2018). A comparison and re-evaluation of the field observations in 2002 (Bárcena et al., 2003) and 2015 (García-Siñeriz et al., 2016) relevant for this work are presented below.

One of the striking features of the bentonite barrier was that most of the swelling and sealing capacity was developed during the first 5 years of heating and hydration, since all the construction gaps in the barrier were completely filled by bentonite, including the 4–5 cm gap at the top of the buffer and the different gaps between blocks, around cable channels, and around sensors. Even the vertical bentonite slices were tightly joined to one another (see Fig. SM-3 in Supplementary Material). The granite/bentonite contact was tight at all locations.

Although the boundaries of the blocks were clearly visible, no gap between them remained after 5 years. Only at the core of the barrier in the cold sections, where the water content had barely increased with respect to the original one, i.e. from 14% to values below 18% (see below) some gaps were open. However, after 18 years of hydration these internal joints were also sealed (Fig. 9); moreover, some joints between blocks of the outer ring were difficult to identify. However, and even in these wettest areas close to the rock, in which the bentonite showed a darker colour reflecting its higher humidity, the blocks could be separated along their borders and showed a considerable mechanical integrity. No mud, gel or free water was observed, except for a local water inflow located at the right hand side of the large lamprophyre dyke (Fig. 1 and Fig. SM-1 in Supplementary Material).

During dismantling, the position of the slices with respect to the origin of the  $x$  coordinate, which was located at the front of the buffer (as indicated in Fig. 1) was measured using laser technology (see Fig. SM-4 in Supplementary Material). The  $x$  coordinates measured in 2002 were mostly shorter than those taken during the construction phase, which means that the barrier “moved” forward. Taking into account the reliability of those measurements, the movements must have been in the range from 2 to 8 cm. The  $x$  coordinates measured in 2015 from the barrier front to the back part of Heater #2 were, as like those of the first dismantling in 2002, shorter than the ones taken during the construction phase. Then, the observations suggest that the buffer, or at least the front of it, expanded towards the entrance of the gallery, which is assumed to have happened as the concrete plug was demolished and the swelling pressure released. However, from the back of Heater #2 towards the back end of the gallery, the  $x$  coordinate decreased from 0 to  $-8$  cm, reflecting the movement of bentonite slices towards the back of the gallery during operation as a result of the higher volume of construction gaps in this part of the barrier (discussed in Villar et al., 2018). Both in 2002 and 2015, small longitudinal grooves in the direction of the gallery axis were observed on the surfaces of bentonite in contact with the rock, and also in the thin film of bentonite that remained adhered to the rock in the already dismantled zones (see Fig. SM-5 in Supplementary Material). These features provide evidence of the barrier movement in this direction.

## 5. Physical state of the barrier

### 5.1. Methodology

About 300 samples of bentonite in 2002 and 424 samples in 2015 were taken in selected vertical sections evenly distributed along the gallery (Fig. 1) for the onsite determination of their dry density and water content. The samples were obtained by core drilling in a direction parallel to the tunnel axis along six radii separated  $60^\circ$ . The samples were immediately wrapped in plastic foil and taken to the onsite laboratory where they were tested at once, to avoid disturbance as much as possible (Daucausse and Lloret, 2003; Villar et al., 2016).

The gravimetric water content ( $w$ ) is defined as the ratio between the mass of water and the mass of dry solid expressed as a percentage. The mass of water was determined as the difference between the mass of the sample and its mass after oven drying at  $110^\circ\text{C}$  (mass of dry solid). Dry density ( $\rho_d$ ) is defined as the ratio between the mass of the dry sample and the volume occupied by it prior to drying. In 2002 to calculate the bulk density of subsamples they were coated in wax and immersed in water. The dry density was calculated using the water content measured in an adjacent subsample. In 2015 the volume of the specimens was determined by immersing them in a vessel containing mercury and by weighing the mercury displaced, considering for the calculation of volume a mercury density of  $13.6\text{ g/cm}^3$ . In this case, the same samples whose volumes had been determined were used for the water content determination.

To compute the water degree of saturation of the bentonite ( $S_r$ ), which is the ratio of volume of water to volume of voids, a density of solid particles ( $\rho_s$ ) of  $2.70 \pm 0.04\text{ g/cm}^3$  was used. This value is that of the FEBEX bentonite used to manufacture the blocks, and is the average of 20 measurements obtained with pycnometers filled with water (Villar, 2002; ENRESA, 2006). In 22 samples taken from Grimsel during the 2015 dismantling, this parameter was determined again and the same average value was found (Villar et al., 2018).

In addition to the uncertainties in the density of solid particles, water content and dry density values determination, there is another reason for computing uncertain degrees of saturation. This is the assumption that the density of water is  $1\text{ g/cm}^3$ , although it is known to be higher in the water adsorbed in bentonites. There is evidence from the fields of neutron diffraction, Monte Carlo computer simulations and quasi-elastic neutron scattering that the density of water attached to

clay minerals may be greater than  $1.0\text{ g/cm}^3$  (Skipper et al., 1991; Monsalvo et al., 2006; Chávez-Páez et al., 2001; Tambach et al., 2004; Huang et al., 1994), with values of water density in phyllosilicates of up to  $1.38\text{ g/cm}^3$ , higher in smectites with divalent cations in the inter-layer (such as FEBEX) than with monovalent ones (Jacinto et al., 2012). This fact becomes more evident in highly compacted expansive clays close to water saturation, in which degrees of saturation much higher than 100% can be computed if a water density value of  $1.0\text{ g/cm}^3$  is considered (Villar, 2002; Marcial, 2003; Lloret and Villar, 2007). Thus, a computed degree of saturation of 115% for a saturated sample would indicate that the average density of the water in it is  $1.15\text{ g/cm}^3$ . Besides, the proportion of adsorbed water (with a density higher than  $1\text{ g/cm}^3$ ) over free water (with a density of  $1\text{ g/cm}^3$ ) increases as the dry density of the bentonite is higher (Pusch et al., 1990), for which reason the degree of saturation computed for saturated samples would be higher the higher their dry density.

Since there is no absolute certainty of the values of water density (which would depend on the particular bentonite, its density and water content), the customary value of  $1\text{ g/cm}^3$  is normally used, which would partially explain the degrees of saturation higher than 100% found in some samples from the second dismantling (Villar et al., 2016). To overcome this uncertainty a simple assumption has been considered in this work. A double porosity structure was assumed, with a microstructure with a constant void ratio ( $e_m = 0.45$ ) (Lloret et al., 2003) where the average water density ( $\rho_{wm}$ ) is  $1.05\text{ g/cm}^3$ , while in the macrostructure the water density ( $\rho_{wM}$ ) is  $1\text{ g/cm}^3$ . The value of the average water density in the microstructure was adjusted considering that the samples located at a distance smaller than 8 cm from the gallery wall were fully saturated. This value is smaller than the average microstructural water density obtained from saturation tests in laboratory (about  $1.2\text{ g/cm}^3$ , Lloret and Villar, 2007) and consequently, the computed degrees of saturation could still be higher than the real ones. The value of the degree of saturation can be calculated from void ratio ( $e$ ) and water content ( $w$ ) using the following equations:

$$w_{xm} = \frac{e_m \rho_{wm}}{\rho_s} \quad (3)$$

$$\text{if } w < w_{xm}: S_r = \frac{w \rho_s}{e \rho_{wm}} \quad (4)$$

$$\text{if } w > w_{xm}: S_r = \frac{e_m}{e} + \frac{(w - w_{xm}) \rho_s}{e \rho_{wM}} \quad (5)$$

where  $w_{xm}$  is the maximum water content in the microstructure.

### 5.2. Results

Some of the sampling sections were located around the heaters, and these will be called in the following “hot sections” whereas those located anywhere else will be called in opposition “cold sections”. Nevertheless this is a simplistic separation, since the temperatures to which the bentonite in each section was subjected varied along the gallery axis (Fig. 3). Thus, among the “hot sections” those located in the middle part of the heaters were hotter than those at the heater ends, whereas among the “cold sections” those towards the ends of the gallery were colder. A distinctive feature of these two groups of sections was that in the “hot sections” the central part was occupied by the heater, whereas in the “cold sections” the core of the barrier was composed by bentonite blocks (Fig. 2).

The water content and dry density in all the sections followed a radial distribution around the axis of the gallery, with the water content decreasing from the granite towards the axis of the gallery and the dry density following the inverse pattern. The six radii sampled in each section yielded very similar water content and dry density distributions, which reveals the radial symmetry around the axis of the gallery for these state properties. This would indicate that natural features

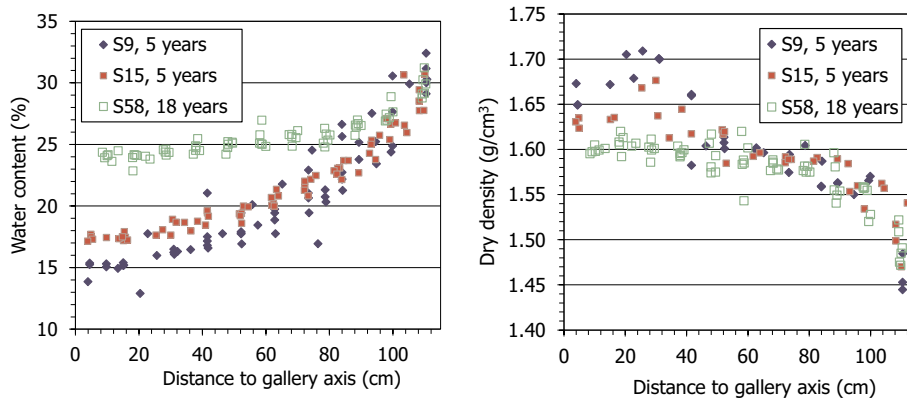


Fig. 10. Water content and dry density of the bentonite barrier along the gallery axis in cold sections after 5 (Daucausse and Lloret, 2003) and 18 years (Villar et al., 2016).

(lamprophyre, fractures) or artefacts resulting from installation particularities that could potentially modify the water input to the bentonite did not systematically affect the water content distribution (Villar et al., 2016).

Fig. 10 shows the water content and dry density determined in the six radii of the “cold” sections in which the temperature was around 22 °C in 2002 and 2015. The water content at 10 cm from the granite in the cold sections was the same after 18 years operation as that after 5 years, whereas the additional operation time allowed for the saturated region to extend farther towards the core of the barrier (left). The Figure also shows the higher water content of section S15 with respect to section S9 after five years, which resulted from the higher temperatures experienced by the latter, which was closer to Heater #1. Provided the temperature is not as high as to cause significant water evaporation and bentonite drying, the permeability increases with temperature (e.g. Ye et al., 2016). This fact accelerated the saturation of the hot sections in the early stages. The saturation and swelling of the external part of the barrier made the dry density decrease very sharply towards the granite (Fig. 10, right). The higher dry density in the core of the barrier of sections S9 and S15 was due to the higher compaction density of the core blocks (block type BB-G-04 and BB-G-05 in Fig. 2, Fuentes-Cantillana and García-Siñeriz, 1998) and to the compression exerted by the external rings of the barrier that were expanding.

The water content and density gradients were more noticeable in those sections affected by the heater, both after 5 and 18 years. In these sections the water content near the granite, i.e. in the external ring of the barrier, decreased from 2002 to 2015. In contrast, during the further 13 years of operation the water content increased in the medium and internal rings of the barrier (Fig. 11, left). Remarkably, the dry

density along the radii around the heaters did not change significantly over time (Fig. 11, right).

Consistently with the water content and dry density distributions, the radial dimensions measured on the surface of the blocks during dismantling indicated the expansion of the external and middle bentonite rings and the compression of the internal one (Villar et al., 2016).

Both after 5 and 18 years the degree of saturation decreased towards the gallery axis, more steeply in the sections around the heaters (Fig. 12, left). This gradient tended to attenuate over time, and in fact, in the cold sections the degree of saturation after 18 years was quite homogeneous and very high in all the sections, with no clear spatial trend. It is noticeable that in many samples the degree of saturation was higher than 100%, the possible reasons being those discussed in 5.1.

From the results presented above and taken into account the radial symmetry of the distribution of the variables, it was possible to compute for each vertical section the average values for the water content ( $w$ ), dry density ( $\rho_d$ ) and degree of saturation ( $S_r$ ) by fitting polynomial functions to represent the variation of these variables with the distance to the gallery axis (Villar et al., 2005, 2018). The water content and dry density values are plotted as a function of the distance to the x-coordinate origin in Fig. 13. The variation of the bentonite installation density along the barrier is also plotted in the Figure. The part of the barrier dismantled in 2002 had an average dry density lower than the part dismantled in 2015 (1.59 vs. 1.61 g/cm<sup>3</sup>, see Table 1). There is not a specific reason for this difference, which is just a consequence of particularities of the installation works.

After 5 years there was a significant overall increase of the barrier water content from the initial value of 14% to an average value of 23%. This increase was homogeneous along the barrier, although the part of

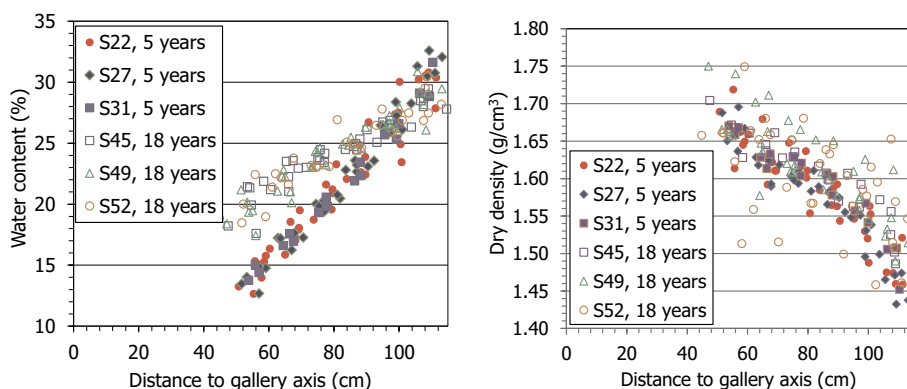


Fig. 11. Water content and dry density of the bentonite barrier along the gallery axis in sections around the heaters after 5 (Daucausse and Lloret, 2003) and 18 years (Villar et al., 2016).

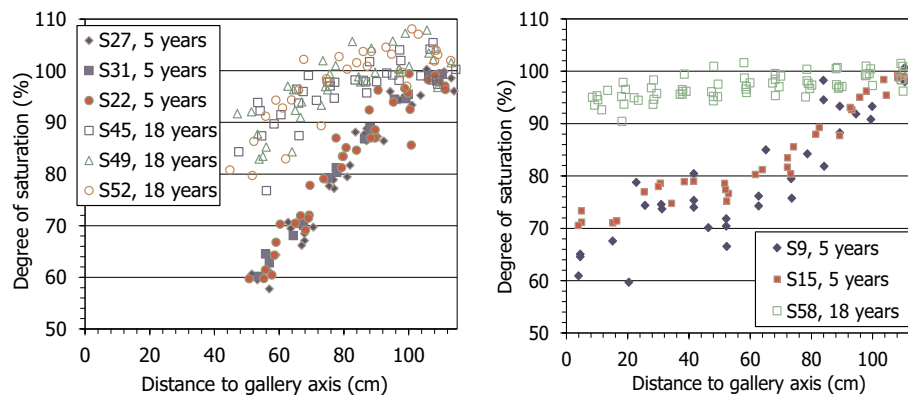


Fig. 12. Degrees of saturation of the bentonite barrier along the gallery axis in sections around the hot (left) and cold (right) sections after 5 (Daucausse and Lloret, 2003) and 18 years (Villar et al., 2016). Computed taking for the water density a value of 1 g/cm<sup>3</sup>.

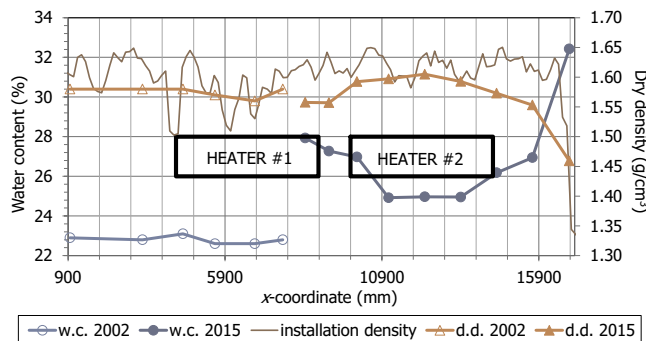


Fig. 13. Average water content (w.c.) and dry density (d.d.) for the sections spanned along the barrier in 2002 and 2015.

Table 1

Average values computed for the first half (2002) and second half (2015) of the barrier.

Dismantling date	w (%)	Installation $\rho_d$ (g/cm <sup>3</sup> )	$\rho_d$ (g/cm <sup>3</sup> )	$S_r$ (%)	Mass of water taken (kg)
2002 <sup>a</sup>	22.9	1.59	1.58	87	4054
2015 <sup>b</sup>	26.7	1.61	1.57	100	6516
2015 <sup>c</sup>	26.9		1.57	97 <sup>d</sup>	

<sup>a</sup> Villar et al. (2005).

<sup>b</sup> Weighing vertical sections.

<sup>c</sup> Global interpolation.

<sup>d</sup> Using a microstructural water density of 1.05 g/cm<sup>3</sup>.

the drift where Heater #1 was placed included a lamprophyre dyke and several other more conductive geological features, such as fissures or dykes which made rock permeability inhomogeneous (Fig. SM-1, Martínez-Landa and Carrera, 2005). This observation shows the predominant control of the bentonite on the hydration kinetics resulting from its much lower permeability with respect to granite (Villar et al., 2005). The effect of the heater was barely remarkable, since the average water content for all the sections, both in cold and hot areas, spanned only between 22.6 and 23.1%, a quite narrow range. The average dry density along the axis of the gallery in the front half of the experiment after 5 years was close to 1.58 g/cm<sup>3</sup> at all points. Only two vertical sections around the middle part of Heater #1 had lower average dry density (1.56 g/cm<sup>3</sup>). These sections coincided with the area of the lamprophyre dyke, where because of the irregularities of the drift many blocks had to be trimmed, causing lower installation density.

The overall increase of water content after the subsequent 13 years of operation was from an average of 23 to 27%, which reflects the slowing down of the hydration rate over time. Furthermore, in this case

the water contents of the sections in hot and cold areas were very different, clearly increasing away from the heater. The average water contents of the different sections spanned between 24.9% around the middle part of Heater #2 to 32.4% at the back of the gallery and 27.9% close to the shotcrete plug. There were also significant longitudinal changes in the average dry density of the sections along the gallery. This longitudinal variability could be mostly explained by three factors (Villar et al., 2016, 2018):

- The barrier at the dead end of the gallery had initially a much lower installation density resulting from the difficulty in filling with bentonite blocks the concave-shaped back of the gallery. The higher volume of voids in this area would make easier for the bentonite to expand towards it as it hydrated, which triggered the density gradient at the back of the gallery. The higher volume of voids would also allow a larger quantity of water to fill them, which, along with the dense fracture system in this part of the gallery (Fig. SM-1), gave place to higher water contents.
- The thermal gradient actually hindered full saturation around Heater #2, and for this reason the average water content in the vertical sections around Heater #2 was lower than in cooler adjacent sections. This is a disparity with respect to the first dismantling, when no significant differences in average water content between hot and cool sections were observed. It would mean that although the thermal gradient had not much influence on the overall initial water intake, it actually hindered saturation in the long term. The reason would be that in the first stages of saturation it was the external ring of the barrier, i.e. the part of it closest to the granite, that took most of the water, and that the temperatures of the external ring in cool and hot sections were too similar to affect noticeably the extent of hydration (between 20 °C in cool areas and 40 °C around the heater, Fig. 4). In fact, the increase in saturated permeability with temperature for the FEBEX bentonite compacted to the range of densities in the barrier was checked to be less than half an order of magnitude (Villar and Gómez-Espina, 2009). However, the temperatures in the middle and internal rings of the barrier, those affected by later hydration stages, were significantly different in cool and hot areas. The temperatures close to the heater were high enough as to trigger the formation of a considerable vapour phase that would move towards cooler areas of the barrier, keeping the proximity to the heater relatively dry for a long time (longer than 18 years).
- The front of the half back part of the barrier was affected by the first dismantling and the construction of the shotcrete plug in 2002, and again in 2015 during the final dismantling. Hence, the decrease in dry density with respect to the installation one observed at the front of Heater #2, around the dummy canister, could have resulted from processes occurred at two different moments: 1) in 2002, when the



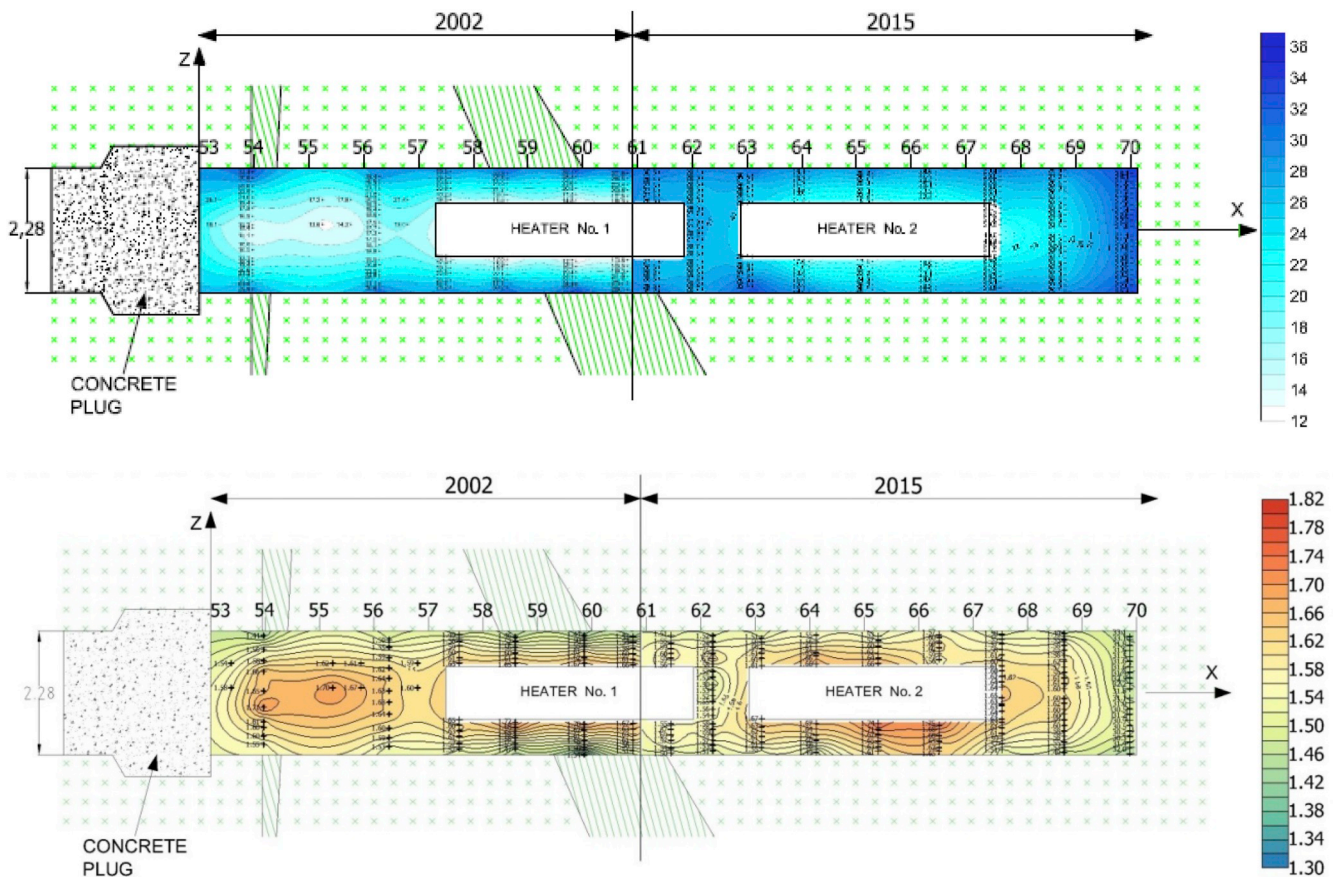


Fig. 14. Contour plots of water content and dry density in 2002 and 2015 in the vertical longitudinal section.

preparation of the bentonite surface that was to be in contact with the shotcrete plug involved some mass loss, and then after the plug installation, because the additional supply of water coming from the shotcrete (reflected in the higher water content of the bentonite in this area) would have made the bentonite swell, pushing towards the back of the gallery, and 2) during dismantling in 2015, because the pressure release upon the concrete plug removal made the bentonite barrier move forward (see Fig. SM-4 in Supplementary Material). The bentonite had also been subjected to high thermal gradient during the 1<sup>st</sup> operational phase but it was cool during the 2<sup>nd</sup> operational phase, which may have also affected its condition.

Using the results of the vertical sampling sections distributed along the axis of the gallery, it was possible to draw contour maps of longitudinal sections along the gallery axis for water content and dry density (Fig. 14). Again, the half front part of the experiment corresponds to the state in 2002 and the half back part to the state in 2015. The same colour codes have been used to plot both. These longitudinal profiles show the lower water content and higher dry density around the heaters and in the core of the cool parts of the barrier highlighted in Fig. 10 and Fig. 11, but also the changes in porosity and water content along the longitudinal direction, away from the heaters' ends, since there was also a thermal gradient from the heaters' ends towards the back and the front of the gallery (Fig. 3). The effect of the longitudinal thermal gradient was evident in the part dismantled in 2015, when the back and front of the barrier had the highest water content and the lowest dry density (although other factors, in addition to the thermal gradient, could have contributed to these differences, as discussed above). But in 2002, when the average degree of saturation of the barrier was not too high, the state of the barrier was quite homogeneous along the axis of the gallery, and the highest gradients in water content

and dry density were observed between the external part of the barrier, close to the granite, and the core of the barrier.

## 6. Assessment of results

The global average water content, dry density and degree of saturation of the first half of the barrier were presented in Villar et al. (2005). Two methods were used to compute these values for the second half of the barrier dismantled in 2015. The first one took into account the volume of the barrier represented by each sampling section (S37 to S61) to compute weighed average values of each parameter. The second one used the software Surfer (Golden Software Inc.) to evaluate the volume of the function  $2\pi r F(x,r)$ , where  $x$  is the longitudinal coordinate,  $r$  is the distance to the gallery axis and  $F$  is the parameter to be averaged. The volume was calculated using the Simpson's 3/8 rule and the function  $F$  was obtained by interpolation over the measured parameters in  $(x,r)$  space using the Kriging gridding method with a linear variogram. According to these values, the best estimates for the final average water content, dry density and degree of saturation of the entire dismantled clay barrier in 2002 and 2015 are shown in Table 1.

The final average dry density measured both in 2002 and 2015 was lower than the installation density of the corresponding part of the barrier (front and back half, respectively). This is attributed to the slight decompression suffered by the barrier during dismantling and to the sampling procedures. The intrusion of bentonite into the void between the perforated liner and the heaters could also have contributed to the decrease in the average dry density of the barrier, particularly in 2015.

The Table also shows the estimated mass of water taken by the two halves of the barrier (front in 2002 and back in 2015), computed from the bentonite mass in place and the final average water contents. These water intakes would roughly correspond to an average water inflow

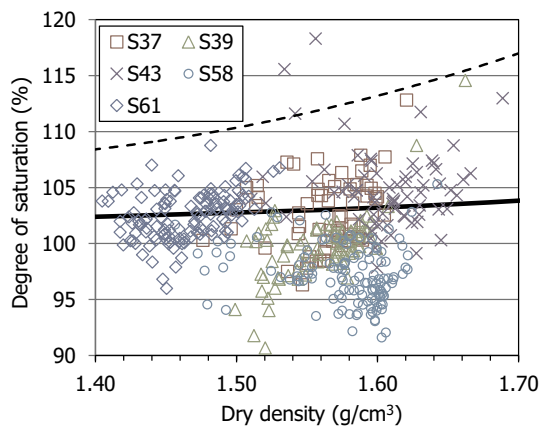


**Fig. 15.** Relationship between degree of saturation (computed with a  $\rho_w$  of  $1\text{ g/cm}^3$ ) and dry density for samples from highly saturated sections after 18 years (a degree of saturation of 105% would mean an average water density of  $1.05\text{ g/cm}^3$ ). The discontinuous line is a fitting for FEBEX samples saturated in the laboratory under constant volume (Villar, 2002; Lloret and Villar, 2007) and the thick line is its modification assuming a microstructural water density of  $1.05\text{ g/cm}^3$ .

into the gallery of  $1.5\text{ mL/min}$  in the period 1997–2002 and of  $0.7\text{ mL/min}$  in the period 2002–2015. Although with a large variability and uncertainty, the groundwater inflow into the gallery measured before placing the bentonite barrier was between 4 and  $9\text{ mL/min}$  (Guimerà et al., 1998). These values show the progressive decrease in the hydration rate and confirm the control of the bentonite on the hydration kinetics (e.g. Alonso et al., 2005), since the granite supplied plenty of water but the bentonite took it at a progressively slower rate.

An interesting feature of the highly saturated parts of the barrier is that the degrees of saturation computed using a water density of  $1\text{ g/cm}^3$  were in many cases (particularly close to the granite) considerably above 100% (Fig. 12), even though, as it has been explained above (subchapter 5.1), because of the sampling and trimming processes the onsite measurements probably underestimated the actual values. In fact, the average degree of saturation computed for the whole barrier would be 100% (Table 1), although the bentonite around the heater was clearly unsaturated. Fig. 15 plots the degrees of saturation against the dry density for sections in which the degree of saturation was high and homogeneous, with no clear trend across the section. In contrast, there was a trend for the computed degree of saturation to increase as the dry density was higher. This agrees with the results obtained from small-scale laboratory tests in which samples of FEBEX bentonite were saturated under isochoric conditions and the degrees of saturation computed using a water density of  $1\text{ g/cm}^3$  were higher as the dry density of the sample was higher, which was interpreted as resulting from the increase of the average water density with clay dry density (Villar, 2002; Villar and Lloret, 2007). This would be a consequence of the predominance of adsorbed water (of higher density) over free water as the density of the clay increases, which is something already stated by Pusch et al. back in 1990 and repeatedly demonstrated since then (e.g. Delage et al., 2006; Matusiewicz et al., 2013; Matusiewicz and Olin, 2019).

The correlation between the computed degrees of saturation and the clay dry density obtained from the small-scale tests mentioned above is also shown in Fig. 15. According to this correlation, for a dry density of  $1.6\text{ g/cm}^3$  (which was the average dry density of the barrier) the average water density in saturated samples would be  $1.14\text{ g/cm}^3$ , which is compatible with an average microstructural water density of  $1.2\text{ g/cm}^3$ . This would mean that the average water content of the barrier once fully saturated would be 29% and that the bentonite from the engineered barrier of the FEBEX test was not yet saturated and could have taken more water. This agrees with the increasing trend of the

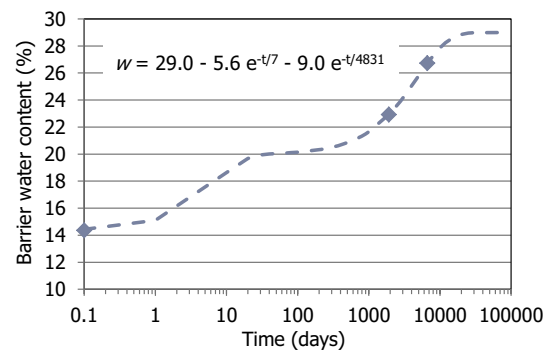


**Fig. 16.** Evolution of the average water content of the barrier over time: values measured in 2002 and 2015 and hypothetical evolution.

pressure sensors located in the barrier (Fig. 6). To compute degrees of saturation compatible with a degree of saturation of 100% for the samples near the gallery (which were saturated) a value of the microstructural water density of  $1.05\text{ g/cm}^3$  was considered in the last row of Table 1 and the resulting correlation between dry density and water content is also shown in Fig. 15.

Villar et al. (2012) found exponential relations between the final water contents of a series of thermo-hydraulic tests in 60-cm long cells performed with FEBEX bentonite blocks and the hydration time. The tests had durations between 6 months and 8 years. Following the same approach, the evolution over time of the barrier average water content has been fit to the same kind of expression. For that, the initial, after-5-years and after-18-years water content values were used, and the maximum water content was fixed to the value of 29% discussed in the previous paragraph (Fig. 16). From this exponential fit the time needed to reach an average water content of 29% would be of about 68 years.

## 7. Summary and concluding remarks

This paper has reported the physical evolution of a bentonite buffer in a simulated nuclear waste underground repository (the FEBEX in situ test at the Grimsel Test Site, Switzerland) over a period of 18 years. Measurements of temperature, pressure and relative humidity supplied online by sensors installed in the bentonite, as well as results of onsite determinations (including water content, dry density, measurement of dimensions and visual inspection) performed during a partial dismantling after 5 years and during the final dismantling after 18 years have been assessed.

The main conditions to which the bentonite buffer was submitted during the whole test operation and until dismantling were:

- the bentonite barrier was hydrated with the groundwater coming from the crystalline host rock for 5 years in the first half part of the experiment and for 18 years in the second half part of it,
- the part of the barrier around the heaters that simulated the waste canisters – whose surface temperature was  $100\text{ }^\circ\text{C}$  – was submitted to a steep thermal gradient for the entire test (5 years around Heater #1 and 18 years around Heater #2),
- the bentonite slices at the front of the gallery surrounding the dummy canister installed during partial dismantling were submitted to thermal gradient during the first five years and then continued hydrating under quasi-isothermal, cooler conditions.

The bentonite dismantling works took several weeks and started after the heaters had been switched off for several days or weeks. During this time the system cooled down and changes took place in the bentonite (see chapter 3). Hence the state observed upon dismantling did not exactly reflect the state of the barrier during the operational phase. The water content of the bentonite close to the heater was lower

during operation than the values measured during dismantling, because of the water transfer caused by cooling (Villar et al., 2005). Conversely, the water content of the middle barrier ring in these areas could have been higher than that measured. These two processes were probably more relevant during the first dismantling, because the degree of saturation close to Heater #1 was lower and, as a result of the higher water potential gradients, the water transfer easier.

In addition to cooling, other processes that could have affected the bentonite before the water content and dry density determinations need to be considered, in particular decompression and expansion of the bentonite upon plug demolition and density decrease induced by sampling and trimming (Villar et al., 2018). For this reason the comparison between the initial and final dry densities shows that the latter were lower (Table 1), although no bentonite mass or overall volume changes took place during operation.

Nonetheless, a comparison of the results obtained in the partial and final dismantlings allows to draw conclusions concerning the saturation rate and the reversibility of the bentonite deformations coupled to hydration and drying. The comparison between the two parts of the experiment (first half dismantled in 2002 and second half dismantled in 2015) is meaningful under the assumption that the conditions of the bentonite around Heater #1 and Heater #2 were analogous, and that the only relevant difference between them was the operation time. However, the two parts of the experiment had clearly distinct hydrogeological conditions, since the lamprophyre dyke around Heater #1 supplied most of the water to the gallery. As it was shown in Gens et al. (2009) and has been confirmed by some of the experimental observations reported here, this fact was irrelevant for the bentonite saturation, whose low permeability controlled the rate of water ingress, which was considerably lower than water inflow into the gallery measured before installation of the barrier and decreased over time during the operational phase.

After 5 years all the construction gaps in the barrier were completely filled by bentonite (see chapter 4). This would mean that the water availability at the test site (both in the liquid and the vapour phase) was enough to allow for quick swelling of the external part of the barrier. In turn, the quick swelling avoided preferential paths to remain open, what made that the water content distribution in vertical sections followed a radial pattern rather independent of the rock particular features or of the block boundaries.

The bentonite vertical sections dismantled after five years of operation had average dry densities that did not change much along the gallery axis. In contrast, the part of the barrier dismantled after 18 years showed considerable longitudinal changes in dry density. These differences were partly inherited from installation, in particular the lower dry density at the back of the gallery, but also resulted from the decompression and stress relief upon plug demolition and dismantling at the front of Heater #2.

The main changes in the period from 2002 to 2015 took place in the internal part of the barrier, its core. This was particularly so around the heaters: the water content and dry density gradients from the granite inwards were steeper in the hot sections than in the cold sections, both after 5 and after 18 years, and despite the overall increase in water content during the further 13 years, the water content gradients did not wane, although they attenuated.

Furthermore, the comparison of the dry density distribution in transversal sections (from granite inwards) after 5 and 18 years, particularly around the heaters (Fig. 11), indicate that the volume changes induced during the initial saturation were irreversible, since the dry density distributions around Heater #1 in 2002 and Heater #2 in 2015 were similar, although changes in water content did take place over time. Based on laboratory tests performed with untreated FEBEX bentonite samples and interpreted by generalised plasticity models (Lloret et al., 2003), Lloret and Villar (2007) stated that, provided that the net stresses in the barrier were not higher than the bentonite swelling pressure, these macroscopic changes would be irreversible and the

density heterogeneity across the barrier would remain (Papafotiou et al., 2017). This would be the case in the FEBEX in situ test, where the net stresses were actually dictated by the swelling pressure developed by the bentonite, since the crystalline rock can be considered rigid. The large swelling deformations in the external part of the barrier caused by the initial water intake seem to have resulted permanent. In fact, the water content and dry density gradients persisted even in sections whose degree of saturation was overall very high in 2015, e.g. section S58 (Fig. 10 and Fig. 12). This is an aspect of consequence for the implementation of planned geological disposal projects for high-level radioactive wastes, since the assessment of long-term safety of a geological repository has to rely on a robust model of the spatial and temporal distribution of the safety relevant properties of bentonite, most of which depend on dry density. Hence, the performance of a permanently inhomogeneous bentonite barrier should be evaluated. The issue is currently a concern for nuclear waste management agencies and the main topic of the project Beacon (<https://www.beacon-h2020.eu/>, Sellin et al., 2019), financed by the European Union. The results presented here –because of its representativeness at the spatial and temporal scales– are a valuable contribution to the conceptual understanding of the long-term mechanical evolution of the bentonite barrier and to enlarge the database on experimental results necessary to verify models.

It is acknowledged that the computed degrees of saturation were lower than the actual ones, because it was difficult to assume a proper water density. The relevance of the water density issue has been put forward, since the water adsorbed in bentonite can reach densities higher than  $1 \text{ g/cm}^3$ , as a result of which the barrier saturation time predicted by standard models can be considerably underestimated.

Considering this evidence along with the results of small and medium-scale laboratory tests and the slowing down of the hydration rate over time, it is speculated that the time needed for full saturation of the FEBEX bentonite barrier would have been longer than 50 years.

None of the observations reported above seems to have compromised the main safety functions of the barrier (swelling capacity and low permeability). Furthermore, the result of 18 years operation was a continuous buffer in which the interfaces between blocks did not have any role on the water content and density distribution or fluid transport. The fact that the barrier could remain unsaturated close to the waste containers for long periods of time does not necessarily mean any impairment of its properties, but may deserve further analysis.

## Declaration of Competing Interest

On behalf of my co-authors I declare that this article has not been published previously, that it is not under consideration for publication elsewhere, that its publication is approved by all authors and tacitly or explicitly by the responsible authorities where the work was carried out, and that, if accepted, it will not be published elsewhere in the same form, in English or in any other language, including electronically without the written consent of the copyright-holder.

There is no conflict of interest in the publication of this paper.

## Acknowledgements

The FEBEX project was financed by ENRESA (Empresa Nacional de Residuos Radiactivos S.A.) and EC Contracts FI4W-CT95-006 and FIKWCT-2000-00016. The Febex-DP Consortium (Nagra, SKB, Posiva, CIEMAT and Kaeri) financed the dismantling operation and on-site determinations in 2015. The Beacon project, which receives funding from the Euratom research and training programme 2014–2018 under grant agreement number 745942, financed the preparation of this paper. Carlos Gutiérrez (CIEMAT) prepared some of the figures.

References<sup>1</sup>

- Alonso, E.E., Alcoverro, J., Coste, F., Malinsky, L., Merrien-Soukatchoff, V., Kadiri, I., Nowak, T., Shao, H., Nguyen, T.S., Selvadurai, A.P.S., Armand, G., Sobolik, S.R., Itamura, M., Stone, C.M., Webb, S.W., Rejeb, A., Tijani, M., Maouche, Z., Kobayashi, A., Kurikami, H., Ito, A., Sujita, Y., CHijimatsu, M., Bergesson, L., Hernelind, J., Rutqvist, J., Tsang, C.-F., Jussila, P., 2005. The FEBEX benchmark test: case definition and comparison of modelling approaches. *Int. J. Rock Mech. Min. Sci.* 42 (5–6), 611–638. <https://doi.org/10.1016/j.ijrmm.2005.03.004>.
- Bárcena, I., Fuentes-Cantillana, J.L., García-Siñeriz, J.L., 2003. Dismantling of the heater 1 at the FEBEX “*in situ*” test. Description of operations. *Publicación Técnica ENRESA 09/2003*, Madrid, pp. 134.
- Bárcena, I., García-Siñeriz, J.L., Huertas, F., 2006. FEBEX Project Final Report. In: Addendum sensors data report. *In situ* experiment. *Publicación Técnica ENRESA 05-5/2006*, Madrid, pp. 157.
- Bernier, F., Neerdael, B., 2007. Overview of in-situ thermomechanical experiments in clay: Concept, results and interpretation. *Eng. Geol.* 41 (1–4), 51–64. [https://doi.org/10.1016/0013-7952\(95\)00032-1](https://doi.org/10.1016/0013-7952(95)00032-1).
- Chávez-Páez, M., Van Workum, K., de Pablo, L., de Pablo, J.J., 2001. Monte Carlo simulations of Wyoming sodium montmorillonite hydrates. *J. Chem. Phys.* 114 (3), 1405–1413. <https://doi.org/10.1063/1.1322639>.
- Daucausse, D., Lloret, A., 2003. Results of “*in situ*” measurements of water content and dry density. In: FEBEX report 70-UPC-L-5-012, pp. 85 Barcelona.
- Delage, P., Marcial, D., Cui, Y.J., Ruiz, X., 2006. Ageing effects in a compacted bentonite: a microstructure approach. *Géotechnique* 56, 291–304. <https://doi.org/10.1680/geot.2006.56.5.291>.
- ENRESA, 1995. Almacenamiento geológico profundo de residuos radiactivos de alta actividad (AGP). In: Diseños conceptuales genéricos. *Publicación Técnica ENRESA 11/95*, Madrid, pp. 105.
- ENRESA, 2006. FEBEX Full-scale Engineered Barriers Experiment, Updated Final Report 1994–2004. *Publicación Técnica ENRESA 05-0/2006*, Madrid, pp. 590.
- Ericsson, L.O., 1999. Geoscientific R&D for high level radioactive waste disposal in Sweden — current status and future plans. *Eng. Geol.* 52 (3–4), 305–317. [https://doi.org/10.1016/S0013-7952\(99\)00013-7](https://doi.org/10.1016/S0013-7952(99)00013-7).
- Fuentes-Cantillana, J.L., García-Siñeriz, J.L., 1998. FEBEX. Final design and installation of the “*in situ*” test at Grimsel. *Publicación Técnica ENRESA 12/98*, Madrid, pp. 184.
- García-Siñeriz, J.L., Villar, M.V., Rey, M., Palacios, B., 2015. Engineered barrier of bentonite pellets and compacted blocks: state after reaching saturation. *Eng. Geol.* 192, 33–45. <https://doi.org/10.1016/j.enggeo.2015.04.002>.
- García-Siñeriz, J.L., Abós, H., Martínez, V., De la Rosa, C. (Aitemin), 2016. FEBEX-DP Dismantling of the heater 2 at the FEBEX “*in situ*” test. NAGRA Arbeitsbereich NAB 16-011, Wettingen, pp. 92.
- Gens, A., Sánchez, M., Guimarães, L.D.N., Alonso, E.E., Lloret, A., Olivella, S., Villar, M.V., Huertas, F., 2009. A full-scale *in situ* heating test for high-level nuclear waste disposal: observations, analysis and interpretation. *Géotechnique* 59 (4), 377–399. <https://doi.org/10.1680/geot.2009.59.4.377>.
- Guimerà, J., Carrera, J., Martínez, L., Vázquez, E., Ortuño, F., Fierz, T., Bühler, C., Vives, L., Meier, P., Medina, A., Saaltink, M., Ruiz, B., Pardillo, J., 1998. Hydrogeological characterization and modeling. In: FEBEX Report 70-UPC-M-1-1001, pp. 106.
- Huang, W.-L., Bassett, W.A., Wu, T.C., 1994. Dehydration and hydration of montmorillonite at elevated temperatures and pressures monitored using synchrotron radiation. *Am. Mineral.* 79, 683–691.
- Jacinto, A., Villar, M.V., Ledesma, A., 2012. Influence of water density on the water-retention curve of expansive clays. *Géotechnique* 62 (8), 657–667. <https://doi.org/10.1680/geot.7.00127>.
- Karland, O., Olsson, S., Sandén, T., Fälth, B., Jansson, M., Eriksen, T.E., Svärdröm, K., Rosborg, B., 2011. Long term test of buffer material at the Äspö HTL, LOT project. Final report on the A0 test parcel. In: Technical Report TR-09-31. Svensk Kärnbränslehantering, Stockholm, pp. 123.
- Lloret, A., Villar, M.V., 2007. Advances on the knowledge of the thermo-hydro-mechanical behaviour of heavily compacted FEBEX bentonite. *Phys. Chem. Earth Parts A/B/C* 32 (8–14), 701–715. <https://doi.org/10.1016/j.pce.2006.03.002>.
- Lloret, A., Villar, M.V., Sanchez, M., Gens, A., Pintado, X., Alonso, E.E., 2003. Mechanical behaviour of heavily compacted bentonite under high suction changes. *Géotechnique* 53 (1), 27–40. <https://doi.org/10.1680/geot.2003.53.1.27>.
- Marcial, D., 2003. Comportement hydromécanique et microstructural des matériaux de barrière ouvragée. Ph.D. Thesis. École Nationale des Ponts et Chaussées, Paris, pp. 316.
- Martínez, V., Abós, H., García-Siñeriz, J.L., 2016. FEBEX: Final Sensor Data Report (FEBEX “*In situ*” Experiment). NAGRA Arbeitsbereich NAB 16-019, Wettingen, pp. 230.
- Martínez-Landa, L., Carrera, J., 2005. An analysis of hydraulic conductivity scale effects in granite (Full-scale Engineered Barrier Experiment (FEBEX), Grimsel, Switzerland). *Water Resour. Res.* 41 (3). <https://doi.org/10.1029/2004WR003458>.
- Matuszewicz, M., Olin, M., 2019. Comparison of microstructural features of three compacted and water saturated swelling clays: MX-80 bentonite, Na- and Ca-purified bentonite. *Clay Miner.* 54 (1), 75–81. <https://doi.org/10.1180/clm.2019.1>.
- Matuszewicz, M., Pirkkalainen, K., Liljeström, V., Suuronen, J.-P., Root, A., Muurinen, A., Serimaa, R., Olin, M., 2013. Microstructural investigation of calcium montmorillonite. *Clay Miner.* 48 (2), 267–276. <https://doi.org/10.1180/claymin.2013.048.2.08>.
- Mokni, N., Barnichon, J.-D., 2016. Hydro-mechanical analysis of SEALEX in-situ tests — Impact of technological gaps on long term performance of repository seals. *Eng. Geol.* 205, 81–92. <https://doi.org/10.1016/j.enggeo.2016.02.013>.
- Monsalvo, R., De Pablo, L., Chávez, M.L., 2006. Hydration of Ca-Montmorillonite at basin conditions: a Monte Carlo molecular simulation. *Rev. Mexic. Cien. Geol.* 23 (1), 84–95.
- Papafotiou, A., Li, C., Kober, F. (Eds.), 2017. Pre-dismantling THM modelling of the FEBEX in situ experiment. NAGRA Arbeitsbereich NAB 16-022, Wettingen, pp. 135.
- Pardillo, J., Campos, R., Guimerà, J., 1997. Caracterización geológica de la zona de ensayo FEBEX (Grimsel - Suiza). In: Informe FEBEX 70-IMA-M-2-01. Madrid/Barcelona, CIEMAT/UPC, pp. 45.
- Pusch, R., Karland, O., Hökmark, H., 1990. GMM - A general microstructural model for qualitative and quantitative studies on smectite clays. In: SKB Technical Report 90-43. Svensk Kärnbränslehantering, pp. 94.
- Sellin, P., Leupin, O., 2013. The use of clays as an engineered barrier in radioactive-waste management — a review. *Clay Clay Miner.* 61 (6), 477–498. <https://doi.org/10.1346/CCMN.2013.0610601>.
- Sellin, P., Westermark, M., Leupin, O., Norris, S., Gens, A., Wiczorek, K., Talandier, J., Swahn, J., 2019. BEACON: bentonite mechanical evolution. *EPJ N Nucl. Sci. Technol* In press.
- Skipper, N.T., Refson, K., McConnell, J.D.C., 1991. Computer simulation of interlayer water in 2:1 clays. *J. Chem. Phys.* 94 (11), 7434–7445. <https://doi.org/10.1063/1.460175>.
- Tambach, T.J., Hensen, E.J.M., Smit, B., 2004. Molecular simulations of swelling clay minerals. *J. Phys. Chem. B* 108 (23), 7586–7596. <https://doi.org/10.1021/jp049799h>.
- Villar, M.V., 2002. Thermo-hydro-mechanical characterisation of a bentonite from Cabo de Gata. A study applied to the use of bentonite as sealing material in high level radioactive waste repositories. *Publicación Técnica ENRESA 01/2002*, Madrid, pp. 258.
- FEBEX Project Final report. In: Villar, M.V. (Ed.), Post-mortem bentonite analysis. 183 *Publicación Técnica ENRESA 05-1/2006*, Madrid.
- Villar, M.V., Gómez-Espina, R., 2009. Report on thermo-hydro-mechanical laboratory tests performed by CIEMAT on FEBEX bentonite 2004-2008. *Informes Técnicos CIEMAT 1178*, Madrid, pp. 67. Agosto 2009. 10.13140/RG.2.2.10087.55208.
- Villar, M.V., Lloret, A., 2007. Dismantling of the first section of the FEBEX *in situ* test: THM laboratory tests on the bentonite blocks retrieved. *Phys. Chem. Earth, Parts A/B/C* 32 (8–14), 716–729. <https://doi.org/10.1016/j.pce.2006.03.009>.
- Villar, M.V., García-Siñeriz, J.L., Bárcena, I., Lloret, A., 2005. State of the bentonite barrier after five years operation of an *in situ* test simulating a high level radioactive waste repository. *Eng. Geol.* 80 (3–4), 175–198. <https://doi.org/10.1016/j.enggeo.2005.05.001>.
- Villar, M.V., Martín, P.L., Bárcena, I., García-Siñeriz, J.L., Gómez-Espina, R., Lloret, A., 2012. Long-term experimental evidences of saturation of compacted bentonite under repository conditions. *Eng. Geol.* 149–150, 57–69. <https://doi.org/10.1016/j.enggeo.2012.08.004>.
- Villar, M.V., Iglesias, R.J., Abós, H., Martínez, V., de la Rosa, C., Manchón, M.A., 2016. FEBEX-DP onsite analyses report. NAGRA Arbeitsbereich NAB 16-019 NAB 16-012, Wettingen, pp. 106.
- Villar, M.V., Iglesias, R.J., García-Siñeriz, J.L., 2018. State of the *in situ* FEBEX test (GTS, Switzerland) after 18 years: a heterogeneous bentonite barrier. *Environ. Geotech.* <https://doi.org/10.1680/jenge.17.00093>.
- Ye, W.M., Wan, M., Chen, B., Chen, Y.G., Cui, Y.J., Wang, J., 2016. Temperature effects on the unsaturated permeability of the densely compacted GMZ01 bentonite under confined conditions. *Eng. Geol.* 126 (13), 1–7. <https://doi.org/10.1016/j.enggeo.2011.10.011>.

<sup>1</sup> The NAB (NAGRA Arbeit Bericht) documents are available through <http://www.grimsel.com/gts-phase-vi/febex-dp/febex-dp-literature-publications>. The SKB documents are available through <https://www.skb.com/publications/>